PHYSICAL REVIEW D **95,** 014010 (2017)

Structure of pentaquarks P_c^+ in the chiral quark model

Gang Yang,[1] Jialun Ping,[1,*] and Fan Wang[2]

[1]*Department of Physics and Jiangsu Key Laboratory for Numerical Simulation of Large Scale Complex Systems, Nanjing Normal University, Nanjing 210023, People's Republic of China*

[2]*Department of Physics, Nanjing University, Nanjing 210093, People's Republic of China*

(Received 6 December 2015; revised manuscript received 13 November 2016; published 10 January 2017)

The recent experimental results of the LHCb Collaboration suggested the existence of pentaquark states with a charmonium. To understand the structure of the states, a dynamical calculation of 5-quark systems with quantum numbers $IJ^P = \frac{1}{2}(\frac{1}{2})^{\pm}$, $\frac{1}{2}(\frac{3}{2})^{\pm}$ and $\frac{1}{2}(\frac{5}{2})^{\pm}$ is performed in the framework of the chiral quark model with the help of the Gaussian expansion method. The results show that there are several negative parity resonance states while all of the positive parity states are the scattering states. The $P_c(4380)$ state is suggested to be the pentaquark state of $\Sigma_c^*\bar{D}$. Although the energy of $\Sigma_c\bar{D}^*$ is very close to the mass of $P_c(4450)$, the inconsistent parity prevents the assignment. The calculated distances between quarks confirm the molecular nature of the states.

DOI: 10.1103/PhysRevD.95.014010

I. INTRODUCTION

The $\Theta^+(1540)$ pentaquark had been reported about 10 years ago by several experimental groups [1–3]. But since JLab reported a high precision negative result [4], almost no one still believes there is such a pentaquark Θ^+ state [LEPS Collaboration still insisted on the existence of a pentaquark $\Theta^+(1540)$ [5]]. However, it does not mean there are no pentaquark components in the usual baryon structure. The valence-sea quark mixing (Fock space expansion) model ($q^3 + q^3q\bar{q}$) of a nucleon ground state has been used to explain the mysterious proton spin structure well [6]. Such a sea quark excitation model has also been used to show that the $q^3q\bar{q}$ excitation is more favorable than the p-wave excitation in the q^3 configuration for $1/2^-$ baryons [7].

Recently, the interest in a pentaquark has been revived, because the LHCb experiment reported the observation of two pentaquark states, denoted as $P_c^+(4380)$ and $P_c^+(4450)$, in the decay of Λ_b^0, $\Lambda_b^0 \to J/\psi K^- p$ [8]. The masses and widths of these two structures, appeared in the $J/\psi p$ invariant mass, are determined to be $4380 \pm 8 \pm 29$ MeV, $205 \pm 18 \pm 86$ MeV, and $4449.8 \pm 1.7 \pm 2.5$ MeV, $39 \pm 5 \pm 19$ MeV. The pentaquark nature of the structures comes from the valence structure, $uudc\bar{c}$, of $J/\psi p$. The most possible quantum numbers J^P of these two states are $(3/2^-, 5/2^+)$ or $(5/2^-, 3/2^+)$. In fact, the hidden-charm pentaquark states have been predicted several years ago. In 2010, J. J. Wu *et al.* predicted several narrow resonances with a hidden charm above 4 GeV, $N^*_{c\bar{c}}(4265)$, $N^*_{c\bar{c}}(4415)$, and $\Lambda^*_{c\bar{c}}(4210)$, in the framework of the coupled-channel unitary approach [9]. Then, a series of calculations using the same method to study the hidden-charm baryons are performed [10]. Z. C. Yang *et al.* also studied the possible existence of very loosely bound hidden-charm molecular baryons in the one-boson-exchange model; $\Sigma_c\bar{D}^*$ and $\Sigma_c\bar{D}$ states are proposed [11]. After the report of LHCb, a lot of theoretical work was devoted to explain the nature of the two states. The interesting features of these two states are the small mass splitting and the decay width; the lower state is broad and the higher one is narrow. By using the boson exchange model, R. Chen *et al.* interpreted the two states as the molecular states, $\Sigma_c(2455)\bar{D}^*$ and $\Sigma_c^*(2520)\bar{D}^*$ with a spin-parity $J^P = 3/2^-$ and $J^P = 5/2^-$, respectively [12]. The Bethe-Salpeter equation method was employed to study the $\bar{D}\Sigma^*$ and $\bar{D}^*\Sigma_c$ interactions, and the two states $P_c^+(4380)$ and $P_c^+(4450)$ are identified as $\Sigma_c^*\bar{D}$ and $\Sigma_c(2455)\bar{D}^*$ molecular states with quantum numbers $J^P = 3/2^-$ and $J^P = 5/2^+$, respectively [13]. The small mass splitting between $P_c^+(4380)$ and $P_c^+(4450)$ is attributed to the heavy quark symmetry limit in these two papers. In the QCD sum rule approach, $P_c^+(4380)$ and $P_c^+(4450)$ were explained as hidden-charm pentaquark states with quantum numbers $J^P = 3/2^-$ and $J^P = 5/2^+$, respectively, by using diquark-diquark-antiquark type interpolating currents [14,15]. By analyzing the reaction $\Lambda_b^0 \to J/\psi K^- p$ with the coupled-channel calculation, L. Roca *et al.* assigned the quantum numbers $J^P = 3/2^-$ to the state $P_c^+(4450)$ and concluded that the $P_c(4450)^+$ state is a molecular state of mostly $\Sigma_c\bar{D}^*$ and $\Sigma_c^*\bar{D}^*$ with $3/2^-$ [16]. In the soliton approach, the hidden-charm state with quantum numbers $IJ^P = \frac{1}{2}\frac{3}{2}^-$ was shown to exist and is compatible with $P_c^+(4380)$, but the state with $IJ^P = \frac{1}{2}\frac{5}{2}^+$ has a much higher mass compared with that of $P_c^+(4450)$ [17]. The small mass splitting between $P_c^+(4380)$ and $P_c^+(4450)$ can be understood in the diquark-triquark model by using an effective diquark-triquark Hamiltonian based on the spin-orbital interaction [18]. Burns studied the model-independent

*Corresponding author.
jlping@njnu.edu.cn

phenomenology of the $P_c^+(4380)$ and $P_c^+(4450)$ pentaquark states based on the meson-baryon molecular configuration; the possible spin-parity assignments of the two states are discussed in detail with the decay patterns and production processes [19]. Nonresonance explanations of the structures observed experimentally were also proposed [20,21]. A detailed review of the experimental progress and theoretical interpretations of the hidden-charm pentaquarks (as well as hidden-charm tetraquark states) can be found in Ref. [22], where the phase space and centrifugal barrier are invoked to explain the small decay width of $P_c^+(4450)$.

Based on the theory of QCD, it is possible to excite quark-antiquark pairs from a vacuum to form a hadronic state. For the light quark-antiquark pair excitation, the effect can be absorbed into the parameters in the quark model description. For the heavy quark-antiquark pair excitation, it is too difficult to occur in the light hadron system, and its effect cannot be absorbed by the model parameters. So the states P_c^+ reported by LHCb should be genuine pentaquarks. Its study will provide us more information of the underlying fundamental theory of the strong interaction, QCD.

The most common approach to a multiquark system is the quark model. After 50 years of development and with the accumulation of experimental data on multiquark states, to tackle the problem of multiquark seriously in the framework of a quark model is expected. In the present work, the chiral quark model is used to study the pentaquark states with a hidden charm. To find the structure of the pentaquark states, a general, powerful method of a few-body system, The Gaussian expansion method (GEM) [23] is employed to do the calculation. The GEM has been successfully applied to many few-body systems, light nuclei, hypernuclei, hadron physics, and so on [23]. It suits for both of the compact multiquark systems and loosely bound molecular states. In this approach, the four relative orbital motions of the system are expanded by Gaussians with various widths. By taking into account all of the possible couplings for color-flavor-spin degrees of freedom, the structure of the system determined by its dynamics can be found.

The structure of the paper is as follows. In Sec. II, the quark model, wave functions, and calculation method are presented. Section III is devoted to the calculated results and discussions. A brief summary is given in the last section.

II. MODEL AND WAVE FUNCTION

The chiral quark model has acquired great achievement both in describing the hadron spectra and hadron-hadron interaction. The details of the model can be found in Ref. [24]. To apply it to a 5-quark system with a hidden charm, the flavor symmetry has to be expanded to SU(4), which has been used to predict the hidden-charm pentaquark states by Wu *et al.* [9] and to study the ND interaction by Haidenbauer *et al.* [25], although it is badly broken. In the present work with no strange quark, flavor symmetry SU(3) is used but with the replacement of a s quark by a c quark. The incorporation of the D-meson exchange is necessary; the decay of pentaquark states P_c^+, the prevailing candidates $\Sigma_c^{(*)}\bar{D}^{(*)}$, to NJ/ψ is through the D-meson exchange. So the Hamiltonian for the present calculation takes the form

$$H = \sum_{i=1}^{n}\left(m_i + \frac{p_i^2}{2m_i}\right) - T_{\rm CM} + \sum_{j>i=1}^{n}\left[V_{\rm CON}(\mathbf{r}_{ij}) + V_{\rm OGE}(\mathbf{r}_{ij}) + V_\chi(\mathbf{r}_{ij}) + V_\sigma^{\rm eff}(\mathbf{r}_{ij})\right], \tag{1}$$

$$V_{\rm CON}(\mathbf{r}_{ij}) = \boldsymbol{\lambda}_i^c\cdot\boldsymbol{\lambda}_j^c[-a_c(1-e^{-\mu_c r_{ij}}) + \Delta],$$

$$V_{\rm OGE}(\mathbf{r}_{ij}) = \frac{1}{4}\alpha_s\boldsymbol{\lambda}_i^c\cdot\boldsymbol{\lambda}_j^c\left[\frac{1}{r_{ij}} - \frac{1}{6m_im_j}\boldsymbol{\sigma}_i\cdot\boldsymbol{\sigma}_j\frac{e^{-r_{ij}/r_0(\mu)}}{r_{ij}r_0^2(\mu)}\right], \qquad r_0(\mu) = \hat{r}_0/\mu, \qquad \alpha_s = \frac{\alpha_0}{\ln(\frac{\mu^2+\mu_0^2}{\Lambda_0^2})},$$

$$V_\chi(\mathbf{r}_{ij}) = v_\pi(\mathbf{r}_{ij})\sum_{a=1}^{3}\boldsymbol{\lambda}_i^a\cdot\boldsymbol{\lambda}_j^a + v_D(\mathbf{r}_{ij})\sum_{a=4}^{7}\boldsymbol{\lambda}_i^a\cdot\boldsymbol{\lambda}_j^a + v_\eta(\mathbf{r}_{ij})[\boldsymbol{\lambda}_i^8\cdot\boldsymbol{\lambda}_j^8\cos\theta_P - \sin\theta_P] \tag{2}$$

$$v_\chi(\mathbf{r}_{ij}) = \frac{g_{ch}^2}{4\pi}\frac{m_\chi^2}{12m_im_j}\frac{\Lambda_\chi^2}{\Lambda_\chi^2 - m_\chi^2}m_\chi\left[Y(m_\chi r_{ij}) - \frac{\Lambda_\chi^3}{m_\chi^3}Y(\Lambda_\chi r_{ij})\right]\boldsymbol{\sigma}_i\cdot\boldsymbol{\sigma}_j. \qquad \chi = \pi, D, \eta$$

$$V_\sigma^{\rm eff}(\mathbf{r}_{ij}) = -\frac{g_{ch}^2}{4\pi}\frac{\Lambda_\sigma^2}{\Lambda_\sigma^2 - m_\sigma^2}m_\sigma\left[Y(m_\sigma r_{ij}) - \frac{\Lambda_\sigma}{m_\sigma}Y(\Lambda_\sigma r_{ij})\right], \tag{3}$$

where $T_{\rm CM}$ is the center of mass kinetic energy, μ is the reduced mass of two interacting quark pairs. According to the nature of the σ meson, it only exchanges between u, d quarks. Because we are interested in the ground state of the multiquark system and to reduce the burden of the calculation, only the central parts of the interactions are employed. All of the symbols take their usual meanings. The model parameters, except Λ_D, are taken from Ref. [24] and are listed in Table I. It is worth mentioning that in the present model, the above quark-quark interaction is

TABLE I. Quark model parameters.

Quark masses	$m_u = m_d$ (MeV)	313
	m_c (MeV)	1752
Goldstone bosons	m_π (fm^{-1})	0.70
	m_η (fm^{-1})	2.77
	Λ_π (fm^{-1})	4.20
	Λ_η (fm^{-1})	5.20
	m_D (fm^{-1})	9.46
	Λ_D (fm^{-1})	17.5
	m_σ (fm^{-1})	3.42
	Λ_σ (fm^{-1})	4.2
	$g_{ch}^2/(4\pi)$	0.54
	$\theta_P(^\circ)$	−15
Confinement	a_c (MeV)	430
	μ_c (fm^{-1})	0.70
	Δ (MeV)	181.10
OGE	α_0	2.118
	Λ_0 (fm^{-1})	0.113
	μ_0 (MeV)	36.976
	$\hat{r}_0$ (MeV fm)	28.170

assumed to be universal according to the "Casimir scaling" [26], independent of the color structures of the multiquark system. The possible multibody interaction in the multiquark system is not considered, although it may give different spectra of multiquark states [27].

The wave functions for the system are constructed in the following way. First, the 5-quark system is separated into two clusters, one with 3 quarks and another with a quark-antiquark. The wave functions for these subclusters can be easily written down. Then two clusters are coupled and antisymmetrized (if necessary) to form the total wave function of a 5-quark system. Clearly, there are other ways to construct the wave functions of the system. However, it makes no difference by choosing any one configuration if all of the possible couplings are considered during the calculation.

For the 5-quark system with the quark content $uudc\bar{c}$, there are two types of separation, one is $(udc)(\bar{c}u) + (uuc)(\bar{c}d)$ and the other is $(uud)(\bar{c}c)$. The flavor wave functions for the subclusters constructed are shown below.

$$
\begin{aligned}
&B_{11} = uuc, \qquad B_{10} = \frac{1}{\sqrt{2}}(ud+du)c, \qquad B_{1-1} = ddc,\\
&B_{00} = \frac{1}{\sqrt{2}}(ud-du)c,\\
&B^1_{\frac{1}{2},\frac{1}{2}} = \frac{1}{\sqrt{6}}(2uud-udu-duu),\\
&B^2_{\frac{1}{2},\frac{1}{2}} = \frac{1}{\sqrt{2}}(ud-du)u,\\
&M_{\frac{1}{2},\frac{1}{2}} = \bar{c}u, \qquad M_{\frac{1}{2},-\frac{1}{2}} = \bar{c}d, \qquad M_{00} = \bar{c}c.
\end{aligned} \tag{4}
$$

The flavor wave functions for the 5-quark system with an isospin $I = 1/2$ are obtained by the following couplings (the states with $I = 3/2$ are not calculated in this work):

$$
\begin{aligned}
\chi^f_1 &= \sqrt{\frac{2}{3}}B_{11}M_{\frac{1}{2},-\frac{1}{2}} - \sqrt{\frac{1}{3}}B_{10}M_{\frac{1}{2},\frac{1}{2}},\\
\chi^f_2 &= B_{00}M_{\frac{1}{2},\frac{1}{2}},\\
\chi^f_3 &= B^1_{\frac{1}{2},\frac{1}{2}}M_{00},\\
\chi^f_4 &= B^2_{\frac{1}{2},\frac{1}{2}}M_{00}.
\end{aligned} \tag{5}
$$

In a similar way, the spin wave functions for a 5-quark system can be constructed,

$$
\begin{aligned}
\chi^{\sigma 1}_{\frac{1}{2},\frac{1}{2}}(5) &= \sqrt{\frac{1}{6}}\chi^\sigma_{\frac{3}{2},-\frac{1}{2}}(3)\chi^\sigma_{11} - \sqrt{\frac{1}{3}}\chi^\sigma_{\frac{3}{2},\frac{1}{2}}(3)\chi^\sigma_{10} + \sqrt{\frac{1}{2}}\chi^\sigma_{\frac{3}{2},\frac{3}{2}}(3)\chi^\sigma_{1-1}\\
\chi^{\sigma 2}_{\frac{1}{2},\frac{1}{2}}(5) &= \sqrt{\frac{1}{3}}\chi^{\sigma 1}_{\frac{1}{2},\frac{1}{2}}(3)\chi^\sigma_{10} - \sqrt{\frac{2}{3}}\chi^{\sigma 1}_{\frac{1}{2},-\frac{1}{2}}(3)\chi^\sigma_{11}\\
\chi^{\sigma 3}_{\frac{1}{2},\frac{1}{2}}(5) &= \sqrt{\frac{1}{3}}\chi^{\sigma 2}_{\frac{1}{2},\frac{1}{2}}(3)\chi^\sigma_{10} - \sqrt{\frac{2}{3}}\chi^{\sigma 2}_{\frac{1}{2},-\frac{1}{2}}(3)\chi^\sigma_{11}\\
\chi^{\sigma 4}_{\frac{1}{2},\frac{1}{2}}(5) &= \chi^{\sigma 1}_{\frac{1}{2},\frac{1}{2}}(3)\chi^\sigma_{00}\\
\chi^{\sigma 5}_{\frac{1}{2},\frac{1}{2}}(5) &= \chi^{\sigma 2}_{\frac{1}{2},\frac{1}{2}}(3)\chi^\sigma_{00}\\
\chi^{\sigma 1}_{\frac{3}{2},\frac{3}{2}}(5) &= \sqrt{\frac{3}{5}}\chi^\sigma_{\frac{3}{2},\frac{3}{2}}(3)\chi^\sigma_{10} - \sqrt{\frac{2}{5}}\chi^\sigma_{\frac{3}{2},\frac{1}{2}}(3)\chi^\sigma_{11}\\
\chi^{\sigma 2}_{\frac{3}{2},\frac{3}{2}}(5) &= \chi^\sigma_{\frac{3}{2},\frac{3}{2}}(3)\chi^\sigma_{00}\\
\chi^{\sigma 3}_{\frac{3}{2},\frac{3}{2}}(5) &= \chi^{\sigma 1}_{\frac{1}{2},\frac{1}{2}}(3)\chi^\sigma_{11}\\
\chi^{\sigma 4}_{\frac{3}{2},\frac{3}{2}}(5) &= \chi^{\sigma 2}_{\frac{1}{2},\frac{1}{2}}(3)\chi^\sigma_{11}\\
\chi^{\sigma 1}_{\frac{5}{2},\frac{5}{2}}(5) &= \chi^\sigma_{\frac{3}{2},\frac{3}{2}}(3)\chi^\sigma_{11}
\end{aligned} \tag{6}
$$

with the spin wave functions for 3-quark and 2-quark subclusters,

$$
\begin{aligned}
\chi^\sigma_{\frac{3}{2},\frac{3}{2}}(3) &= \alpha\alpha\alpha,\\
\chi^\sigma_{\frac{3}{2},\frac{1}{2}}(3) &= \frac{1}{\sqrt{3}}(\alpha\alpha\beta+\alpha\beta\alpha+\beta\alpha\alpha),\\
\chi^\sigma_{\frac{3}{2},-\frac{1}{2}}(3) &= \frac{1}{\sqrt{3}}(\alpha\beta\beta+\beta\alpha\beta+\beta\beta\alpha),\\
\chi^{\sigma 1}_{\frac{1}{2},\frac{1}{2}}(3) &= \frac{1}{\sqrt{6}}(2\alpha\alpha\beta-\alpha\beta\alpha-\beta\alpha\alpha),\\
\chi^{\sigma 2}_{\frac{1}{2},\frac{1}{2}}(3) &= \frac{1}{\sqrt{2}}(\alpha\beta\alpha-\beta\alpha\alpha),\\
\chi^{\sigma 1}_{\frac{1}{2},-\frac{1}{2}}(3) &= \frac{1}{\sqrt{6}}(\alpha\beta\beta-\alpha\beta\beta-2\beta\beta\alpha),\\
\chi^{\sigma 2}_{\frac{1}{2},-\frac{1}{2}}(3) &= \frac{1}{\sqrt{2}}(\alpha\beta\beta-\beta\alpha\beta),\\
\chi^\sigma_{11} &= \alpha\alpha, \qquad \chi^\sigma_{10} = \frac{1}{\sqrt{2}}(\alpha\beta+\beta\alpha), \qquad \chi^\sigma_{1-1} = \beta\beta,\\
\chi^\sigma_{00} &= \frac{1}{\sqrt{2}}(\alpha\beta-\beta\alpha).
\end{aligned}
$$

For the color wave function, not only the color singlet channels ($k=1$), but also the hidden color channels ($k=2,\ 3$), are used here. In principle, the color-singlet channels form a complete set for the multiquark system if all the possible excitations are considered. The fact is pointed out by Harvey in studying the nucleon-nucleon interaction [28]. Wang proved it for multiquark system [29]. It is also demonstrated in the dynamical calculation of a four-quark system [30] recently. However, to use the colorless hadrons to describe a multiquark system is not an economic way because the whole tower of physical states needs to be taken into account. For example, to study the four-quark states with diquark-antidiquark structure, using the combination of a color singlet and the hidden color of $q\bar{q}-q\bar{q}$ is much cheaper than using the whole tower of colorless mesons. So in the present calculation, the color singlet and hidden-color channels are employed. Then the color wave functions of the system are

$$\chi_1^c=\frac{1}{\sqrt{18}}(rgb-rbg+gbr-grb+brg-bgr)\times(\bar{r}r+\bar{g}g+\bar{b}b), \tag{7}$$

$$\chi_k^c=\frac{1}{\sqrt{8}}(\chi_{3,1}^k\chi_{2,8}-\chi_{3,2}^k\chi_{2,7}-\chi_{3,3}^k\chi_{2,6}+\chi_{3,4}^k\chi_{2,5}+\chi_{3,5}^k\chi_{2,4}-\chi_{3,6}^k\chi_{2,3}-\chi_{3,7}^k\chi_{2,2}+\chi_{3,8}^k\chi_{2,2}), \tag{8}$$

with $k=2,\ 3$ and

$$\chi_{3,1}^2=\frac{1}{\sqrt{6}}(2rrg-rgr-grr),\qquad \chi_{3,1}^3=\frac{1}{\sqrt{2}}(rgr-grr),$$
$$\chi_{3,2}^2=\frac{1}{\sqrt{6}}(rgg+grg-2ggr),\qquad \chi_{3,2}^3=\frac{1}{\sqrt{2}}(rgg-grg),$$
$$\chi_{3,3}^2=\frac{1}{\sqrt{6}}(2rrb-rbr-brr),\qquad \chi_{3,3}^3=\frac{1}{\sqrt{2}}(rbr-brr),$$
$$\chi_{3,4}^2=\frac{1}{\sqrt{12}}(2rgb-rbg+2grb-gbr-brg-bgr),$$
$$\chi_{3,4}^3=\frac{1}{\sqrt{4}}(rbg+gbr-brg-bgr),$$
$$\chi_{3,5}^2=\frac{1}{\sqrt{4}}(rbg-gbr+brg-bgr),$$
$$\chi_{3,5}^3=\frac{1}{\sqrt{12}}(2rgb+rbg-2grb-gbr-brg+bgr),$$
$$\chi_{3,6}^2=\frac{1}{\sqrt{6}}(2ggb-gbg-bgg),\quad \chi_{3,6}^3=\frac{1}{\sqrt{2}}(gbg-bgg),$$
$$\chi_{3,7}^2=\frac{1}{\sqrt{6}}(rbb+brb-2bbr),\quad \chi_{3,7}^3=\frac{1}{\sqrt{2}}(rbb-brb),$$
$$\chi_{3,8}^2=\frac{1}{\sqrt{6}}(gbb+bgb-2bbg),\quad \chi_{3,8}^3=\frac{1}{\sqrt{2}}(gbb-bgb),$$

$$\chi_{2,1}=\bar{b}r,\qquad \chi_{2,2}=\bar{b}g$$
$$\chi_{2,3}=-\bar{g}r,\qquad \chi_{2,4}=\frac{1}{\sqrt{2}}(\bar{r}r-\bar{g}g),$$
$$\chi_{2,5}=\frac{1}{\sqrt{6}}(2\bar{b}b-\bar{r}r-\bar{g}g),\qquad \chi_{2,6}=\bar{r}g$$
$$\chi_{2,7}=-\bar{g}b,\qquad \chi_{2,8}=\bar{r}b.$$

As for the orbital wave functions, we do not separate the motions of particles in the system into internal and relative ones and freeze the internal motion, as most work did. In the present work, the orbital wave functions for each relative motion of the system are determined by the dynamics of the system, The orbital wave functions for this purpose are obtained as follows:

$$\psi_{LM_L}=[[[\phi_{n_1l_1}(\boldsymbol{\rho})\phi_{n_2l_2}(\boldsymbol{\lambda})]_l\phi_{n_3l_3}(\boldsymbol{r})]_{l'}\phi_{n_4l_4}(\boldsymbol{R})]_{LM_L}, \tag{9}$$

where the Jacobi coordinates are defined as

$$\boldsymbol{\rho}=\boldsymbol{x}_1-\boldsymbol{x}_2,$$
$$\boldsymbol{\lambda}=\boldsymbol{x}_3-\left(\frac{m_1\boldsymbol{x}_1+m_2\boldsymbol{x}_2}{m_1+m_2}\right),$$
$$\boldsymbol{r}=\boldsymbol{x}_4-\boldsymbol{x}_5,$$
$$\boldsymbol{R}=\left(\frac{m_1\boldsymbol{x}_1+m_2\boldsymbol{x}_2+m_3\boldsymbol{x}_3}{m_1+m_2+m_3}\right)-\left(\frac{m_4\boldsymbol{x}_4+m_5\boldsymbol{x}_5}{m_4+m_5}\right). \tag{10}$$

To find the orbital wave functions, the Gaussian expansion method (GEM) is employed, i.e., every ϕ is expanded by Gaussians with various sizes [23]

$$\phi_{nlm}(\boldsymbol{r})=\sum_{n=1}^{n_{\max}}c_nN_{nl}r^le^{-(r/r_n)^2}Y_{lm}(\hat{r}), \tag{11}$$

where N_{nl} are normalization constants

$$N_{nl}=\left[\frac{2^{l+2}(2\nu_n)^{l+\frac{3}{2}}}{\sqrt{\pi}(2l+1)}\right]^{\frac{1}{2}}. \tag{12}$$

The size parameters of Gaussians r_n are taken as the geometric progression numbers

$$r_n=r_{\min}a^{n-1}. \tag{13}$$

c_n is the variational parameters, which is determined by the dynamics of the system. Finally, the complete channel wave function for the 5-quark system is written as

$$\Psi_{JM,i,j,k,n}=\mathcal{A}[[\chi_S^{\sigma_i}(5)\psi_L]_{JM}\chi_j^f\chi_k^c], \tag{14}$$

where the $\mathcal{A}$ is the antisymmetry operator of the system; it has ten terms for the system with four identical particles,

and it can be reduced to five terms, as follows, due to the symmetry between the first two particles that has been considered when constructing the wave functions of the 3-quark clusters.

$$\mathcal{A} = 1 - (13) - (23) - (15) - (25). \tag{15}$$

The eigenenergy of the system is obtained by solving the following eigenequation:

$$H\Psi_{JM} = E\Psi_{JM}, \tag{16}$$

by using variational principle. The eigenfunctions Ψ_{JM} are the linear combinations of the above channel wave functions.

When the angular momenta are not all zero, the calculation of the matrix elements of the Hamiltonian is rather complicated. Here, a useful method named the infinitesimally shifted Gaussian is used [23]. In this method, the spherical harmonic function is absorbed into the shifted Gaussians,

$$\phi_{nlm}(\boldsymbol{r}) = N_{nl}\lim_{\varepsilon\to 0}\frac{1}{(\nu\varepsilon)^l}\sum_{k=1}^{k_{\max}} C_{lm,k}e^{-\nu_n(\boldsymbol{r}-\varepsilon D_{lm,k})^2}; \tag{17}$$

the calculation becomes easy with no tedious angular-momentum algebra required.

III. RESULTS AND DISCUSSIONS

In the present calculation, we are interested in the low-lying states of the $uudc\bar{c}$ pentaquark system, so the total orbital angular momentum L is limited to be 0 and 1. For $L = 0$, all of the l_1, l_2, l_3, l_4 are 0, and for $L = 1$, only one of l_1, l_2, l_3, l_4 can be 1. In this way, the total angular momentum J can take the values of $1/2$, $3/2$, and $5/2$. The possible channels under the consideration are listed in Table II.

First, the single channel calculations are performed. The eigenenergies and distances between any two quarks for resonance states are shown in Tables III, IV, and V. Tables III and IV give the eigenenergies of the states (column 3), along with the theoretical (column 4) and experimental thresholds (column 6), the binding energies (column 5), the difference between the eigenenergies and the theoretical threshold and the corrected energies of the states (column 7), which are obtained by taking the sum of experimental thresholds and the binding energies. Table V gives the spacial configurations of the states. The color singlet ($k = 1$) results are similar to that of other quark model calculations (e.g., [11]). For $N\eta_c$, NJ/ψ, $\Lambda_c\bar{D}$, and $\Lambda_c\bar{D}^*$ channels, the lowest energy of each channel is close to but higher than the corresponding threshold, respectively, whereas for $\Sigma_c\bar{D}$, $\Sigma_c\bar{D}*$, $\Sigma_c^*\bar{D}$, and $\Sigma_c^*\bar{D}^*$ channels, the lowest energy of each channel is below the corresponding threshold, the resonances (these states that can couple to the states with lower energies, e.g., $N\eta_c$, NJ/ψ, $\Lambda_c\bar{D}$) are possible. The distances between quarks show that the consistent pictures for the color-singlet resonances are molecules. For the hidden-color channels ($k = 2$, 3), all the channels, except $\Sigma_c^*\bar{D}^*$ with $J^P = 1/2^-$, have higher energies than the corresponding color-singlet states. The results infer that the color excitation (hidden-color channels) generally exhausts more energies.

TABLE II. The channels under consideration.

J^P	$1/2^-$	$\frac{3}{2}^-$	$\frac{5}{2}^-$
(L,S)	$(0,\frac{1}{2})$	$(0,\frac{3}{2})$	$(0,\frac{5}{2})$
J^P	$\frac{1}{2}^+$	$\frac{3}{2}^+$	$\frac{5}{2}^+$
(L,S)	$(1,\frac{1}{2})$, $(1,\frac{3}{2})$	$(1,\frac{1}{2})$, $(1,\frac{3}{2})$, $(1,\frac{5}{2})$	$(1,\frac{3}{2})$, $(1,\frac{5}{2})$

Secondly, the three types of channel coupling calculations are performed. The first is the channel coupling between color-singlet and hidden-color channels with the same flavor-spin structures. The second is the coupling among all color-singlet channels with different flavor-spin structures, and the last is the full coupling, including all channels for a given J^P. In performing the channel-coupling calculation by including open-charm and closed-charm channels, the spurious states will appear, which are removed by the eigenvalue method. By diagonalizing the overlap matrix of the system and removing the eigenvectors with eigenvalue zero, the spurious states are removed. From the results, we can see that the coupling between color-singlet and hidden-color states is very weak for octet baryon-pseudoscalar meson channels, strong for decuplet baryon-vector meson channels, and lies in between for other channels. In the following, we analyze the results in detail.

(a) $J^P = \frac{1}{2}^-$: For $N\eta_c$, NJ/ψ, $\Lambda_c\bar{D}$, and $\Lambda_c\bar{D}^*$ states, the single-channel calculation shows that no bound state can be formed. For $\Sigma_c\bar{D}$, $\Sigma_c\bar{D}*$, and $\Sigma_c^*\bar{D}$ states, the single channel calculation show that the energy of the system is -3–-4 MeV lower than the corresponding threshold. Coupling to the corresponding hidden-color channel, the energy of the system is pushed down further, 4 MeV for $\Sigma_c\bar{D}$, 39 MeV for $\Sigma_c\bar{D}^*$, and 102 MeV for $\Sigma_c^*\bar{D}$. Coupling all the color-singlet channels together, the lowest energy is 3745 MeV, the theoretical threshold of $N\eta_c$. So the channel coupling does not push the state $N\eta_c$ or $\Lambda_c\bar{D}$ down enough to form a bound state. The full channel coupling does not change this result. This result is different from the results of Ref. [31], where the channel coupling made the state $N\eta_c$ bound. In the full channel coupling calculation, although there is no bound state, the resonances are possible. By changing the place of the boundary, we found that there are several energy fluctuations around several energies. For example, by changing $r_{n_{\max}}$ from 6 fm to 8 fm, there is always an eigenstate with an energy between 4392 and 4396; the dominant component of the state is $\Sigma_c\bar{D}$. The

TABLE III. The lowest eigenenergies of the $udc\bar{c}u$ system with $J^P = \frac{1}{2}^-$ (unit: MeV). The percentages of color-singlet (S) and hidden-color (H) channels are also given.

Channel	E	$E_{\rm th}^{\rm Theo}$	E_B	$E_{\rm th}^{\rm Exp}$	E'
$\chi_{1/2}^{\sigma i}\chi_j^f\chi_k^c$ $i=4,5$, $j=3,4$, $k=1$	3745	3745	0	3919 ($N\eta_c$)	3919
$\chi_{1/2}^{\sigma i}\chi_j^f\chi_k^c$ $i=4,5$, $j=3,4$, $k=2,3$	4714				
color singlet + hidden color	3745				
$\chi_{1/2}^{\sigma i}\chi_j^f\chi_k^c$ $i=2,3$, $j=3,4$, $k=1$	3841	3841	0	4036 (NJ/ψ)	4036
$\chi_{1/2}^{\sigma i}\chi_j^f\chi_k^c$ $i=2,3$, $j=3,4$, $k=2,3$	4964				
color singlet + hidden color	3841				
$\chi_{1/2}^{\sigma i}\chi_j^f\chi_k^c$ $i=4,5$, $j=2$, $k=1$	3996	3996	0	4151 ($\Lambda_c\bar{D}$)	4151
$\chi_{1/2}^{\sigma i}\chi_j^f\chi_k^c$ $i=4,5$, $j=2$, $k=2,3$	4663				
color singlet + hidden color	3996				
$\chi_{1/2}^{\sigma i}\chi_j^f\chi_k^c$ $i=2,3$, $j=2$, $k=1$	4115	4115	0	4293 ($\Lambda_c\bar{D}^*$)	4293
$\chi_{1/2}^{\sigma i}\chi_j^f\chi_k^c$ $i=2,3$, $j=2$, $k=2,3$	4599				
color singlet + hidden color	4115				
$\chi_{1/2}^{\sigma i}\chi_j^f\chi_k^c$ $i=4,5$, $j=1$, $k=1$	4398	4402	−4	4320 ($\Sigma_c\bar{D}$)	4316
$\chi_{1/2}^{\sigma i}\chi_j^f\chi_k^c$ $i=4,5$, $j=1$, $k=2,3$	4835				
color singlet + hidden color	4394	4402	−8	4320	4312
			Percentage(S;H): 91.0%; 7.0%		
$\chi_{1/2}^{\sigma i}\chi_j^f\chi_k^c$ $i=2,3$, $j=1$, $k=1$	4518	4520	−2	4462 ($\Sigma_c\bar{D}^*$)	4460
$\chi_{1/2}^{\sigma i}\chi_j^f\chi_k^c$ $i=2,3$, $j=1$, $k=2,3$	4728				
color singlet + hidden color	4479	4520	−41	4462	4421
			percentage(S;H): 67.4%; 32.6%		
$\chi_{1/2}^{\sigma i}\chi_j^f\chi_k^c$ $i=1$, $j=1$, $k=1$	4563	4566	−3	4527 ($\Sigma_c^*\bar{D}^*$)	4524
$\chi_{1/2}^{\sigma i}\chi_j^f\chi_k^c$ $i=1$, $j=1$, $k=2,3$	4476				
color singlet + hidden color	4461	4566	−105	4527	4422
			percentage(S;H): 23.0%; 77.0%		
Mixed (only color singlet)	3745				
Mixed (color singlet + hidden color)	3745				

results may imply that a resonance $\Sigma_c\bar{D}$ appears. The result is in agreement with that of Ref. [11]. To make a further check, the $N\eta_c$ scattering calculation with a channel coupling is needed. We have similar results for $\Sigma_c\bar{D}*$ and $\Sigma_c^*\bar{D}$ states.

(b) $J^P = \frac{3}{2}^-$: Similar results with the case of $J^P = \frac{1}{2}^-$ are obtained. NJ/ψ, $\Lambda_c\bar{D}^*$ states are unbound, and the energies of all $\Sigma_c\bar{D}$'s are below their corresponding thresholds. The channel coupling to the hidden color pushes down the states, 1 MeV for $\Sigma_c\bar{D}$, 12 MeV for $\Sigma_c\bar{D}^*$, and 15 MeV for $\Sigma_c^*\bar{D}$. No bound state appears in the full channel coupling calculation. Resonances are also possible, especially the resonance $\Sigma_c^*\bar{D}$ that has the mass 4382 MeV after the correction, which is very close to the mass of $P_c^+(4380)$, which was claimed by the LHCb Collaboration [1]. However, the large decay width of $P_c^+(4380)$ cannot be explained in the present calculation. The decay width of the $\Sigma_c^*\bar{D}$ state to NJ/ψ, $\Lambda_c\bar{D}^*$ are estimated to several MeVs from the channel coupling calculation. Because of the missing of the spin-orbit interaction in the present calculation, the energies of NJ/ψ, $\Sigma_c\bar{D}^*$ with $J^P = \frac{3}{2}^-$ are the same as that of $\Sigma_c\bar{D}^*$, NJ/ψ with $J^P = \frac{1}{2}^-$ in the single channel calculation.

(c) $J^P = \frac{5}{2}^-$: Only one channel: $\Sigma_c^*\bar{D}^*$ remains in this case if all orbital angular momenta are set to zero. A resonance state is obtained as before. Although the energy of the state is only −3 MeV lower than the threshold, the decay width of the state may be small, estimated to be 10–20 MeV, due to the weak coupling to $\Lambda_c\bar{D}$, $\Sigma_c\bar{D}$, etc. (tensor interaction induced) and the small decay widths of its constituents, $\Sigma_c^*(\Gamma_{\Sigma_c^*\to\Lambda_c\pi} \sim 15$ MeV) and $\bar{D}^*(\Gamma_{\bar{D}^*\to\bar{D}\pi} \sim 1$ MeV). So it is a good candidate of the heavy pentaquark with high spin.

To find the structure of the resonances obtained in the present work, the distances between any two quarks are calculated. The results for single channel calculations are shown in Table V. For the color-singlet channel, the distances are about 0.8–0.9 fm between light quarks (u, d), and 0.7–0.8 fm between the light quark and charm quark, whereas the distances between the quark (light and charm) and antiquark are rather large, 2.1–2.6 fm. Clearly,

TABLE IV. The lowest eigenenergies of the $udc\bar{c}u$ system with $J^P = \frac{3}{2}^-$ and $\frac{5}{2}^-$ (unit: MeV).

Channel	E	$E_{\rm th}^{\rm Theo}$	E_B	$E_{\rm th}^{\rm Exp}$	E'
$J^P = 3/2^-$					
$\chi_{3/2}^{\sigma i}\chi_j^f\chi_k^c$ $i=3,4, j=3,4, k=1$	3841	3841	0	4036 (NJ/ψ)	4036
$\chi_{3/2}^{\sigma i}\chi_j^f\chi_k^c$ $i=3,4,$ $j=3,4,$ $k=2,3$	4722				
color singlet + hidden color	3841				
$\chi_{3/2}^{\sigma i}\chi_j^f\chi_k^c$ $i=3,4,$ $j=2,$ $k=1$	4115	4115	0	4293 ($\Lambda_c\bar{D}^*$)	4293
$\chi_{3/2}^{\sigma i}\chi_j^f\chi_k^c$ $i=3,4,$ $j=2,$ $k=2,3$	4680				
color singlet + hidden color	4115				
$\chi_{3/2}^{\sigma i}\chi_j^f\chi_k^c$ $i=3,4,$ $j=1,$ $k=1$	4518	4520	−2	4462 ($\Sigma_c\bar{D}^*$)	4460
$\chi_{3/2}^{\sigma i}\chi_j^f\chi_k^c$ $i=3,4,$ $j=1,$ $k=2,3$	4961				
color singlet + hidden color	4517	4520	−3	4462	4459
			Pcentage(S;H): 96.3%; 3.7%		
$\chi_{3/2}^{\sigma i}\chi_j^f\chi_k^c$ $i=2,$ $j=1,$ $k=1$	4444	4447	−3	4385 ($\Sigma_c^*\bar{D}$)	4382
$\chi_{3/2}^{\sigma i}\chi_j^f\chi_k^c$ $i=2,$ $j=1,$ $k=2,3$	4754				
color singlet + hidden color	4432	4447	−15	4385	4370
			Percentage(S;H): 82.6%; 17.4%		
$\chi_{3/2}^{\sigma i}\chi_j^f\chi_k^c$ $i=1,$ $j=1,$ $k=1$	4564	4566	−2	4527 ($\Sigma_c^*\bar{D}^*$)	4525
$\chi_{3/2}^{\sigma i}\chi_j^f\chi_k^c$ $i=1,$ $j=1,$ $k=2,3$	4623				
color singlet + hidden color	4549	4566	−17	4527	4510
			Percentage(S;H): 61.1%; 38.9%		
Mixed (only color singlet)	3841				
Mixed (color singlet + hidden color)	3841				
$J^P = 5/2^-$					
$\chi_{5/2}^{\sigma i}\chi_j^f\chi_k^c$ $i=1,$ $j=1,$ $k=1$	4563	4566	−3	4527 ($\Sigma_c^*\bar{D}^*$)	4524
$\chi_{5/2}^{\sigma i}\chi_j^f\chi_k^c$ $i=1,$ $j=1,$ $k=2,3$	5002				
color singlet + hidden color	4477	4566	−89	4527	4438
			percentage(S;H): 66.2%; 33.8%		

TABLE V. Distances between any two quarks (unit: fm).

J^P	Channel	r_{12}	r_{13}	r_{14}	r_{34}
$\frac{1}{2}^-$	$\chi_{1/2}^{\sigma i}\chi_j^f$ $i=4,5,$ $j=1,$ $k=1$ ($\Sigma_c\bar{D}$)	0.8	0.7	2.1	2.1
	$\chi_{1/2}^{\sigma i}\chi_j^f$ $i=4,5,$ $j=1,$ $k=2,3$	1.0	0.8	0.8	0.4
	$\chi_{1/2}^{\sigma i}\chi_j^f$ $i=2,3,$ $j=1,$ $k=1$ ($\Sigma_c\bar{D}^*$)	0.8	0.7	2.2	2.1
	$\chi_{1/2}^{\sigma i}\chi_j^f$ $i=2,3,$ $j=1,$ $k=2,3$	0.9	0.8	0.8	0.4
	$\chi_{1/2}^{\sigma i}\chi_j^f$ $i=1,$ $j=1,$ $k=1$ ($\Sigma_c^*\bar{D}^*$)	0.9	0.8	2.1	2.0
	$\chi_{1/2}^{\sigma i}\chi_j^f$ $i=1,$ $j=1,$ $k=2,3$	0.9	0.8	0.8	0.4
$\frac{3}{2}^-$	$\chi_{3/2}^{\sigma i}\chi_j^f$ $i=3,4,$ $j=1,$ $k=1$ ($\Sigma_c\bar{D}^*$)	0.8	0.7	2.4	2.3
	$\chi_{3/2}^{\sigma i}\chi_j^f$ $i=3,4,$ $j=1,$ $k=2,3$	1.1	0.9	0.9	0.5
	$\chi_{3/2}^{\sigma i}\chi_j^f$ $i=2,$ $j=1,$ $k=1$ ($\Sigma_c^*\bar{D}$)	0.9	0.8	2.2	2.2
	$\chi_{3/2}^{\sigma i}\chi_j^f$ $i=2,$ $j=1,$ $k=2,3$	1.0	0.9	0.9	0.5
	$\chi_{3/2}^{\sigma i}\chi_j^f$ $i=1,$ $j=1,$ $k=1$ ($\Sigma_c^*\bar{D}^*$)	0.9	0.8	2.6	2.4
	$\chi_{3/2}^{\sigma i}\chi_j^f$ $i=1,$ $j=1,$ $k=2,3$	0.9	0.9	0.8	0.4
$\frac{5}{2}^-$	$\chi_{5/2}^{\sigma i}\chi_j^f$ $i=1,$ $j=1,$ $k=1$ ($\Sigma_c^*\bar{D}^*$)	0.9	0.8	2.4	2.3
	$\chi_{5/2}^{\sigma i}\chi_j^f$ $i=1,$ $j=1,$ $k=2,3$	1.3	1.4	1.3	0.8

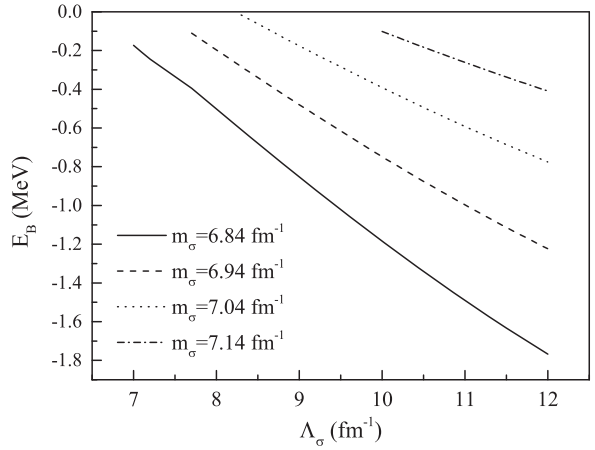

FIG. 1. The binding energy of states with $IJ^P = \frac{1}{2}\frac{3}{2}^+$ and $\frac{1}{2}\frac{5}{2}^+$ as a function of the mass of a σ meson and cutoff Λ_σ.

the molecular structure is shown up. For the hidden color channel, the distances are 0.8–1.1 fm between quarks (light and charm, a little larger, 1.3–1.4 fm for $J^P = 5/2^-$ states), and between the light quark and antiquark. Meanwhile, the distance between the charm quark and anticharm quark is rather small, 0.4–0.5 fm (a little larger, 0.8 fm for $J^P = 5/2^-$ states). In this case, the pattern is that the charm-anticharm quarks form a compact core, and the light quarks move around the core, a genuine pentaquark state. However, the main component of the resonances are a color-singlet state; the structure of pentaquark resonances in the present calculation is molecular one.

For the parity positive states, only one of the orbital angular momenta is set to 1 in the present calculation. The single channel calculations show that the energies of all the states under investigation are higher than the corresponding thresholds. Inspired by the previous calculations of $X(3872)$, the channel coupling between the open-charm ($D\bar{D}^*$) and closed-charm ($\omega J/\psi$) channels are important to form the state [32], the full channel-coupling calculation, including the open-charm and the closed-charm channels, are performed. Unfortunately, the repulsive nature of the closed-charm channel and the weak channel coupling deny the existence of the pentaquark state. So in the present version of the model, the attraction is not enough to make the parity positive state bound. The reason for the deficiency of the attraction comes from the σ-meson exchange, which provide a universal attraction, is missing between heavy-heavy quarks and heavy-light quarks. For the system with heavy quarks, the scalar nonet exchange should be used instead of the σ-meson exchange. However, there are too few scalar meson in the charm sector. So we approximated the effect of the scalar nonet by an effective single scalar exchange potential, as Garcilazo *et al.* did in Ref. [33]. The mass and the cutoff of the effective scalar are taken as parameters. Using the effective σ meson, we recalculate the parity positive states, $IJ^P = \frac{1}{2}\frac{3}{2}^+$ and $\frac{1}{2}\frac{5}{2}^+$, the channel coupling results show that a very weakly bound state is possible (see Fig. 1). However the results are model dependent. More studies on the scalar meson exchange are needed to clarify the situation. So if the state $P_c^+(4450)$ is identified as a pentaquark state with a positive parity, the scalar meson exchange between heavy-light and heavy-heavy quarks has to be taken into account in the chiral quark model. The nonresonance explanation of the narrow structure at 4.45 GeV was also proposed, Guo *et al.* showed that the structure was compatible with the kinematical effects of the rescattering from $\chi_{c1}p$ to $J/\psi p$ [21].

IV. SUMMARY

In the framework of the chiral quark model, the 5-quark systems with quark contents $uddc\bar{c}$ are investigated by means of the Gaussian expansion method. The calculation shows that there are several resonances for $IJ^P = \frac{1}{2}\frac{3}{2}^-, \frac{1}{2}\frac{3}{2}^-$, and $\frac{1}{2}\frac{5}{2}^-$, in which the mass of the state $\frac{1}{2}\frac{3}{2}^-$ with the configuration $\Sigma_c^*\bar{D}$ is very close to that of the state $P_c^+(4380)$, a pentaquark announced by the LHCb Collaboration. The distances between quark pairs suggest a molecular structure for these resonances. A sound interpretation of $P_c^+(4380)$ is the molecule of $\Sigma_c^*\bar{D}$ with $IJ^P = \frac{1}{2}\frac{3}{2}^-$. However, the large decay width of $P_c^+(4380)$, $205 \pm 18 \pm 86$ MeV, is out of reach of the present picture. The mass of the molecule state $\Sigma_c\bar{D}^*$ with $IJ^P = \frac{1}{2}\frac{1}{2}^-$ or $\frac{1}{2}\frac{3}{2}^-$ is also close to that of $P_c^+(4450)$, another pentaquark reported by the LHCb Collaboration. Nevertheless, the opposite parity of the state to the $P_c^+(4380)$ may prevent this assignment. Meanwhile, all the positive parity states are all unbound in our calculation, unless the effective σ-meson exchange is employed.

Channel coupling is a mechanism to form a bound state, it has been applied to explain the formation of $X(3872)$ by E. Swanson [34] and T. Fernández-Caramés *et al.* [35]. The possible dibaryon state H particle is also attributed to the channel coupling [36]. Recently, $N\eta_c$ and NJ/ψ are also shown to be bound under the channel coupling [31]. However, the channel coupling does not bring us any bound state in the present calculation. The reason for this phenomenon is that the attraction is too weak for the states because the σ meson is missing between heavy-light and heavy-heavy quarks.

In the present calculation, the internal structures of the subclusters are not fixed, the structure of a 5-quark system is determined by the dynamics of the system, because all the possible coupling are included except the high orbital angular momentum. In the same framework of the quark model, generally the state in this approach will have a smaller energy than it in other approaches, because of the larger Hilbert space used. The effect of high orbital angular momenta needs a further check [37].

As a preliminary work, the spin-orbit and tensor interactions are not included in the calculation. For parity

negative states, their effects are expected to be zero or small. For the parity positive state, it may play a crucial role because the mass of $P_c^+(4450)$ is very close to threshold of $\chi_{c1}(1P)p$. To understand the nature of $P_c^+(4450)$ in the quark model approach, the calculation that includes the spin-orbit interaction is needed, which is in progress in our group.

The quark model is a phenomenogical approach to the hadron physics. It has been successfully applied to describe the hadron properties and hadron-hadron interaction, where the color structure is almost unique. However, the success depends on the availability of a large amount of experimental data. Applying the quark model to a multiquark system, where abundant color structures are shown up, different versions of the quark model give different descriptions, especially if a lot of predictions of multiquark states are proposed. Unfortunately, almost no state is confirmed by experiments so far. Nevertheless, as a convenient and useful tool, the quark model needs to be developed by incorporating new ingredients. With the accumulation of experimental data on a multiquark state, the effectiveness of the quark model description is expected to increase.

ACKNOWLEDGMENTS

The work is supported partly by the National Natural Science Foundation of China under Grants No. 11535005, No. 11175088, and No. 11205091.

[1] T. Nakano *et al.* (LEPS Collaboration), Phys. Rev. Lett. **91**, 012002 (2003).
[2] V. V. Barmin *et al.* (DIANA Collaboration), Yad. Fiz. **66**, 1763 (2003) [Phys. At. Nucl. **66**, 1715 (2003)].
[3] S. Stepanyan *et al.* (CLAS Collaboration), Phys. Rev. Lett. **91**, 252001 (2003).
[4] M. Battaglieri *et al.* (CLAS Collaboration), Phys. Rev. Lett. **96**, 042001 (2006), and references therein.
[5] T. Nakano *et al.* (LEPS Collaboration), Phys. Rev. C **79**, 025210 (2009).
[6] D. Qing, X. S. Chen, and F. Wang, Phys. Rev. C **57**, R31 (1998); Phys. Rev. D **58**, 114032 (1998).
[7] B. S. Zou, Chin. Phys. C **33**, 1113 (2009).
[8] R. Aaij *et al.* (LHCb Collaboration), Phys. Rev. Lett. **115**, 072001 (2015).
[9] J. J. Wu, R. Molina, E. Oset, and B. S. Zou, Phys. Rev. Lett. **105**, 232001 (2010); Phys. Rev. C **84**, 015202 (2011).
[10] J. J. Wu, T. S. H. Lee, and B. S. Zou, Phys. Rev. C **85**, 044002 (2012); C. Garcia-Recio, J. Nieves, O. Romanets, L. L. Salcedo, and L. Tolos, Phys. Rev. D **87**, 074034 (2013); C. W. Xiao, J. Nieves, and E. Oset, Phys. Rev. D **88**, 056012 (2013).
[11] Z. C. Yang, Z. F. Sun, J. He, X. Liu, and S. L. Zhu, Chin. Phys. C **36**, 6 (2012).
[12] R. Chen, X. Liu, X. Q. Li, and S. L. Zhu, Phys. Rev. Lett. **115**, 132002 (2015).
[13] J. He, Phys. Lett. B **753**, 547 (2016).
[14] H. X. Chen, W. Chen, X. Liu, T. G. Steel, and S. L. Zhu, Phys. Rev. Lett. **115**, 172001 (2015).
[15] Z. G. Wang, Eur. Phys. J. C **76**, 70 (2016).
[16] L. Roca, J. Nieves, and E. Oset, Phys. Rev. D **92**, 094003 (2015).
[17] N. N. Scoccola, D. O. Riska, and M. Rho, Phys. Rev. D **92**, 051501 (2015).
[18] R. L. Zhu and C. F. Qiao, Phys. Lett. B **756**, 259 (2016).
[19] T. J. Burns, Eur. Phys. J. A **51**, 152 (2015).
[20] X. H. Liu, Q. Wang, and Q. Zhao, Phys. Lett. B **757**, 231 (2016).
[21] F. K. Guo, U. G. Meißner, W. Wang, and Z. Yang, Phys. Rev. D **92**, 071502 (2015).
[22] H. X. Chen, W. Chen, X. Liu, and S. L. Zhu, Phys. Rep. **639**, 1 (2016).
[23] E. Hiyama, Y. Kino, and M. Kamimura, Prog. Part. Nucl. Phys. **51**, 223 (2003).
[24] J. Vijande, F. Fernandez, and A. Valcarce, J. Phys. G **31**, 481 (2005).
[25] J. Haidenbauer, G. Krein, U.-G. Meißner, and L. Tolos, Eur. Phys. J. A **47**, 18 (2011).
[26] G. S. Bali, Phys. Rev. D **62**, 114503 (2000).
[27] J.-M. Richard, Phys. Rev. C **81**, 015205 (2010); M. W. Paris, Phys. Rev. Lett. **95**, 202002 (2005); C. R. Deng, J. L. Ping, F. Wang, and T. Goldman, Phys. Rev. D **82**, 074001 (2010).
[28] M. Harvey, Nucl. Phys. **A352**, 301 (1981); **A352**, 326 (1981).
[29] F. Wang, Progress in Physics **9**, 297 (1989).
[30] J. Vijande, A. Valcarce, and N. Barnea, Phys. Rev. D **79**, 074010 (2009); J. Vijande and A. Valcarce, Phys. Rev. C **80**, 035204 (2009); D. Janc and M. Rosina, Few-Body Syst. **35**, 175 (2004).
[31] H. X. Huang, C. R. Deng, J. L. Ping, and F. Wang, Eur. Phys. J. C **76**, 624 (2016).
[32] E. Swanson, Phys. Lett. B **588**, 189 (2004); T. Fernandez-Carames, A. Valcarce, and J. Vijande, Phys. Rev. Lett. **103**, 222001 (2009).
[33] H. Garcilazo, T. Fernandez-Carames, and A. Valcarce, Phys. Rev. C **75**, 034002 (2007).
[34] E. S. Swanson, Phys. Lett. B **588**, 189 (2004).
[35] T. Fernández-Caramés, A. Valcarce, and J. Vijande, Phys. Rev. Lett. **103**, 222001 (2009).
[36] H. R. Pang, J. L. Ping, F. Wang, T. Goldman, and E. G. Zhao, Phys. Rev. C **69**, 065207 (2004).
[37] J. Vijande, E. Weissman, N. Barnea, and A. Valcarce, Phys. Rev. D **76**, 094022 (2007).